

Ultrasonic attenuation in amorphous silicon at 50 and 100 GHz

D. B. Hondongwa and B. C. Daly

Vassar College Physics and Astronomy Department Poughkeepsie, New York 12604, USA

T. B. Norris

Center for Ultrafast Optical Science University of Michigan Ann Arbor, Michigan 48105, USA

B. Yan, J. Yang, and S. Guha

Uni-Solar Ovonic LLC Troy, Michigan 48084, USA

(Received 14 January 2011; published 10 March 2011)

We have measured the attenuation of longitudinal acoustic waves in a series of amorphous and nanocrystalline silicon films using picosecond ultrasonics. The films were grown using a modified very high frequency glow discharge method on steel substrates. The deposition conditions were similar to that used in the fabrication of high-efficiency solar cells. The film thicknesses were varied so we could distinguish between interface losses and intrinsic losses within the silicon films. We determine the attenuation of amorphous Si to be $780 \pm 160 \text{ cm}^{-1}$ at 100 GHz and $340 \pm 120 \text{ cm}^{-1}$ at 50 GHz, values that are lower than those predicted by theories based on anharmonic interactions of the sound wave with localized phonons or extended resonant modes. We determine the attenuation of nanocrystalline Si at 50 GHz to be nearly an order of magnitude higher than amorphous Si ($2600 \pm 660 \text{ cm}^{-1}$) and compare that value to a simple Rayleigh scattering prediction.

DOI: [10.1103/PhysRevB.83.121303](https://doi.org/10.1103/PhysRevB.83.121303)

PACS number(s): 68.60.Bs, 43.35.+d, 62.80.+f, 65.60.+a

The attenuation of high-frequency sound waves in amorphous materials is not yet well understood. This is not surprising considering the uncertainty that remains in the study of the thermal conductivity of amorphous materials, a topic that is directly related. In this rapid communication, we report picosecond ultrasonic measurements of ultrasound attenuation at 50 and 100 GHz at room temperature in thin films of hydrogenated amorphous Si (a-Si:H) grown on stainless steel substrates. The attenuation of ultrasound in amorphous silicon has received theoretical attention,¹ but to our knowledge, no measurements in the GHz regime have been made in order to contribute to the discussion. Several experimental^{2,3} and theoretical⁴ studies have been made of the thermal conductivity of a-Si and a-Si:H, including very recent reports of anomalously high thermal conduction in hot wire chemical vapor deposited (HWCVD) samples.^{5,6} In all cases, analysis of the thermal conductivity measurements typically boils down to an attempt to determine the overall magnitude and frequency dependence of the lifetime of long-wavelength (~ 1 THz) acoustic phonons or localized phonon-like excitations. It is envisioned that the accurate measurements of attenuation in the subterahertz regime that are possible using the technique of picosecond ultrasonics will assist in the overall picture of thermal transport in amorphous materials. The measurements presented in this communication will also facilitate future picosecond ultrasonic studies of mechanical properties of a-Si:H and nanocrystalline silicon (nc-Si:H) films that are used in high-efficiency solar cells. Toward that end, we have also measured the attenuation in nc-Si:H and find an order of magnitude larger attenuation of 50-GHz ultrasound as compared with a-Si:H.

The samples were grown using a modified very high frequency (VHF) glow discharge method at a high deposition rate on steel substrates. The deposition conditions were similar to that used in the deposition of high-efficiency solar cells.⁷

A proper hydrogen dilution with an H_2 and SiH_4 mixture was used to improve the material quality. A series of samples with different thicknesses was made under the same deposition conditions, such as substrate temperature, gas flow rates, pressures, and VHF power. The deposition time was varied to achieve designed film thicknesses. For nc-Si:H deposition, a high hydrogen dilution and dilution profiling were used to control the crystallinity along the growth direction.⁸ The crystalline volume fraction and grain size can be controlled by the dynamical change of H_2 and SiH_4 flow rates.⁹ The nc-Si:H films used in this study were deposited under the condition of best nc-Si:H solar cell performance. Under this condition, a uniform crystalline volume fraction was demonstrated by Raman and cross-sectional TEM (X-TEM) measurements with roughly 50% Raman-determined crystalline volume fraction. X-ray diffraction (XRD) showed a (220) preferential orientation with grain size around 20–30 nm. Thin aluminum layers for use as transducers were deposited on the top surface of the a-Si:H layers using a thermal evaporation method.

To measure the attenuation we used the now well-established technique of picosecond ultrasonics^{10,11} and specifically followed the methods described by Morath and Maris in a 1996 article.¹² A diode laser-pumped Ti : sapphire oscillator (Coherent Mira) that operates at a repetition rate of 76 MHz and emits pulses that are ~ 100 fs in duration was used to perform the optical pump and probe experiment. Pump and probe beams with average power ~ 10 mW were focused down to the same ~ 15 - μm diameter spot on the Al-coated silicon film samples. The absorption of pump pulses caused rapid thermal expansion of the Al transducer layer, which launched longitudinal acoustic pulses into the Si film. The acoustic pulses are roughly single cycle with the compressive strain leading the rarefactive strain, and they contain a broad range of frequencies of coherent long-wavelength acoustic phonons. We used Al transducer thicknesses of 30 and 15 nm

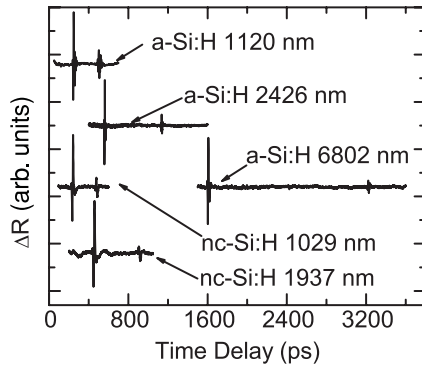


FIG. 1. Change in reflectivity ΔR versus delay time for three a-Si:H and two nc-Si:H samples. The data are offset for clarity and the thermal background has been subtracted from each data set.

in order to obtain variation of the central acoustic frequency generated. The 30-nm films provided measurable frequencies (well above the noise floor) for a-Si:H in the range of 30–90 GHz while the 15-nm films provided measurable frequencies ranging from 40 to 120 GHz. The strain pulses were detected by time-delayed optical probe pulses that are sensitive to changes in the reflectivity, ΔR of the Al film.

Figure 1 shows ΔR versus delay time for three a-Si:H samples and two nc-Si:H samples of varying thicknesses. For this graph, the initial electronic response of the Al film near 0 ps has been removed for all five sets of data, as has the thermal decay of the reflectivity change. The signals that remain for each data set represent the detection of two acoustic pulses: one that has traveled a complete round trip through the Si film and back to the Al transducer after reflecting from the steel substrate and one that has made two such round trips. The time delay between the two signals can be used to accurately measure the thickness of the Si film if a value of the sound velocity is assumed. The five data sets have all been normalized to have the same amplitude of the first signal $\Delta R_1(t)$ so one can get a sense of the reduction in amplitude of the second signal $\Delta R_2(t)$ in each case. Two effects are immediately observable from this graph. First, the overall attenuation of the signal is significantly affected by increasing the thickness of the samples. Second, the attenuation is much larger in the nc-Si:H, as despite using significantly thinner samples, we observe a comparable reduction in the size of $\Delta R_2(t)$.

To obtain quantitative results for the attenuation α as a function of the frequency ω , we obtained the Fourier transforms of each of the signals and calculated their ratio, $\Delta R_1(\omega)/\Delta R_2(\omega)$, as was done in Ref. 12. In Fig. 2 we plot this ratio at 50 and 100 GHz for measurements taken on six a-Si:H samples coated with 15-nm Al transducers as a function of the sample thickness. In analyzing this graph, it is important to note that the acoustic loss represented by this ratio is caused by multiple factors, not simply the intrinsic attenuation in the a-Si:H that we wish to measure. There is a reflection loss that occurs at the Si-steel interface, as some part of the acoustic wave will propagate into the steel rather than return to the free surface to be detected by the optical probe pulses. In addition, there may be losses due to imperfections at the Si-steel interface or the Al-Si interface as well. Rather than attempt to calculate these losses, we choose to obtain an

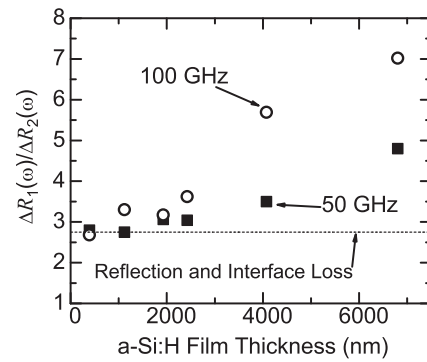


FIG. 2. Ratio of the Fourier transform amplitude of signal 1 to signal 2 at 50 GHz (■) and 100 GHz (○) for six a-Si:H samples of varying thickness. The reflection and interface losses are determined experimentally and are indicated by the dashed line at 2.75. All loss above this line is considered to be intrinsic to the a-Si:H.

experimental value by analyzing the results of Fig. 2. The value of the ratio does not deviate significantly from ~ 3 until the two thickest samples are considered. The implication here is that at thicknesses of roughly 2000 nm or less, the attenuation is dominated by the reflection and interface losses. For the two thickest samples, however, we find that there is enough of an increase in the attenuation that the component of attenuation due to the a-Si:H itself can be measured.

We then calculate α using the expression:

$$\alpha = \frac{1}{d} \ln \left(\frac{r \Delta R_1(\omega)}{\Delta R_2(\omega)} \right), \quad (1)$$

where d is the round trip distance through the film and r is an experimentally determined reflection coefficient that also includes the losses described above. From the data of Fig. 2 and repeated measurements on the 15- and 30-nm Al transducer samples, we find a value of $r = 0.36$ for a-Si:H, and this is represented in Fig. 2 as a dashed line at a ratio of $(0.36)^{-1} = 2.75$. No frequency dependence of this effect was observed. As a comparison, we can also calculate a value of r from the acoustic mismatch between the a-Si:H and the steel using the expression $r = (\rho_{\text{Steel}} v_{\text{Steel}} - \rho_{\text{Si}} v_{\text{Si}}) / (\rho_{\text{Steel}} v_{\text{Steel}} + \rho_{\text{Si}} v_{\text{Si}})$. Using literature values of $\rho_{\text{Steel}} = 7.9 \text{ g/cm}^3$, $v_{\text{Steel}} = 5790 \text{ m/s}$,¹³ $\rho_{\text{Si}} = 2.3 \text{ g/cm}^3$,¹⁴ and $v_{\text{Si}} = 8400 \text{ m/s}$ ¹⁵ we find $r = 0.41$, just slightly larger than our experimentally determined value. We note that the longitudinal sound velocity in a-Si:H has been variously reported as low as 7600 m/s and as high as 8500 m/s, but as the deposition methods of Ref. 15 are nominally most similar to our methods, we have chosen the value from that reference. The value for d is measured by using this value of v_{Si} and the picosecond ultrasonic data illustrated in Fig. 1.

Using Eq. (1) and values of $\Delta R_1(\omega)/\Delta R_2(\omega)$ from 4072- and 6800-nm-thick a-Si:H films we find $\alpha = 340 \pm 120 \text{ cm}^{-1}$ at 50 GHz and $780 \pm 160 \text{ cm}^{-1}$ at 100 GHz. The uncertainties were determined from repeated measurements made using the 15- and 30-nm transducer samples and include the uncertainty in the experimental value of r . The values are about an order of magnitude smaller than those reported for other amorphous materials,¹² including a-SiO₂, which was most recently reported by Devos *et al.* to have an attenuation

of 18000 cm^{-1} at 219 GHz.¹⁶ That the amorphous phase of Si should have a lower GHz attenuation than many other amorphous materials is not entirely surprising, as the 2002 review of low-temperature thermal conductivity and internal friction by Pohl, Liu, and Thompson certainly indicates that the fourfold coordinated materials tend to demonstrate weaker anharmonicity.¹⁷ Our measured values are higher than recently reported values for crystalline Si (74 cm^{-1} at 20 GHz, 87 cm^{-1} at 50 GHz, and 119 cm^{-1} at 100 GHz)^{18,19} but are within an order of magnitude. While our measured attenuation indicates a linear dependence on frequency, the uncertainties are such that a quadratic dependence is by no means ruled out by our measurement.

Theoretical predictions of acoustic attenuation in amorphous solids generally agree that at room temperature, a quadratic frequency dependence is expected in the frequency range of 10 GHz–1 THz and its origins are expected to be the anharmonicity of the interatomic bonds. This has certainly been observed in previous experimental work on a-SiO₂ and other amorphous thin films using picosecond ultrasonics^{12,16} or Brillouin light scattering.^{20,21} At lower frequencies, thermally activated relaxation is expected to dominate.²² The attenuation in amorphous solids at frequencies above 1 THz is naturally linked with the study of thermal transport, and at present this topic is still a matter of considerable debate and experimental investigation. It has long been theorized that the universal plateau in the thermal conductivity of amorphous solids in the temperature range from a few K up to 20 or 30 K could be explained by a dramatic increase in the attenuation ($\alpha \propto \omega^4$ or larger) as the Ioffe-Regel limit (when the phonon mean free path approaches the phonon wavelength) is reached.²³ Examples of recent investigations include a 2008 inelastic x-ray scattering measurement²⁴ of THz vibrational damping in amorphous SiO₂ that found $\alpha \propto \omega^2$ and a similar study in²⁵ 2010 that yielded $\alpha \propto \omega^4$.

In Fig. 3 we plot our measured values for the attenuation along with predictions for a-Si from the work of Fabian and Allen.¹ In that work, the authors appealed to a model of attenuation based on the work of Akhiezer,²⁶ in which the sound wave causes the local thermal vibrations (phonons or phononlike “vibrons”) to be displaced from equilibrium. The sound wave loses energy as these vibrational states return to their original occupation numbers. They used a 3D 1000-atom simulation employing realistic atomic coordinates and interatomic potentials in order to calculate the mode Gruneisen parameters to be used in a relaxation-time approximation calculation.²⁷ Their calculations for the attenuation of ultrasound in a-Si are represented in Fig. 3 and are in reasonable agreement with our results. The complete model of Fabian and Allen includes the effect of the internal strain caused by the randomized atomic positions in the amorphous model. The presence of the internal strain, in turn, causes some low-frequency resonant modes in softer, undercoordinated regions of the amorphous Si network to have very large negative Gruneisen parameters (as low as -30),²⁸ and these large values are responsible for much of the attenuation. Their model overestimates our measured attenuation by about a factor of 6 at both 50 and 100 GHz. Also plotted in Fig. 3 is the calculation of Fabian and Allen when the internal

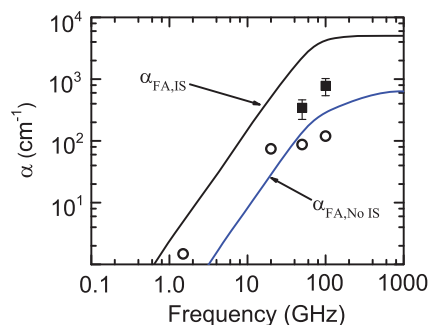


FIG. 3. Measured attenuation versus frequency for a-Si:H (■). Literature values for attenuation in c-Si (○) as reported in Refs. 18 and 19. $\alpha_{\text{FA,IS}}$ and $\alpha_{\text{FA,No IS}}$ are from Ref. 1 and represent the attenuation calculated with and without internal strain.

strain effect is eliminated from the simulation. Our measured values fall directly between the values calculated with and without internal strain. It is interesting to note that better agreement appears to occur between the calculation without internal strain and the published values for the attenuation of crystalline Si,^{18,19,29} despite the random network structure of the numerical model.

In attempting to compare the theoretical predictions of Ref. 1 with our data, a few limitations must be noted. First, the calculation ignores the contribution of thermal transport from compressive to rarefying regions of longitudinal waves that is typically included in the Akhiezer loss, and therefore 100 GHz is expected to be the upper limit of that model’s predictive power. Second, the model calculation was performed for a-Si, not a-Si:H, and the hydrogen content for our samples is estimated at 15%. While thermal conductivity results have been shown to have no significant dependence on H content from 1 to 20%,² it is possible that clusters of H atoms may have an impact on the coordination of the amorphous Si network, contributing to changes in the Gruneisen parameters discussed above. Future measurements of attenuation of a-Si:H with varying H content should be able to shed light on this issue. Last, we point out that while theoretical models of an amorphous material can provide a truly random network, a recent study of electron nanodiffraction patterns from a sputtered a-Si sample indicated that much of that sample was in fact composed of Si crystallites of 1-2 nm.³⁰

Another model of high frequency sound wave damping in amorphous materials is the fracton model: a microscopic model that suggests that below a certain length scale, glasses exhibit a fractal structure but that beyond that scale, the structure can be considered to be homogeneous.^{31–33} This provides for the existence of extended phonon modes at frequencies lower than some cutoff frequency ω_C but localized modes called “fractons” above ω_C . While direct evidence of a fractal microscopic structure in bulk or thin film amorphous materials has not been found, the theory remains a very powerful one, due to its ability to predict properties of glasses using essentially no free parameters. In Eq. 7 of Ref. 12 and its subsequent text, Morath and Maris have presented a simple calculation of the attenuation of a long-wavelength phonon of frequency ω via an anharmonic (three-“phonon”) interaction with a localized fracton mode. The attenuation

at room temperature is proportional to ω^2 and depends only on the material parameters ω_C and κ_{HOP} —the contribution to the thermal conductivity at room temperature due only to the hopping of fractons. These two parameters can be established for a-Si by analyzing the low-temperature plateau region of thermal conductivity data for the amorphous material. Using the thermal conductivity data of Ref. 2 we find that the fracton theory overestimates our measured the attenuation by a factor of 20 at 50 GHz and a factor of 40 at 100 GHz. This is somewhat poorer than the comparison found for other amorphous films in Ref. 12, but it should be noted that published low-temperature thermal conductivity data for a-Si and a-Si:H vary with fabrication methods. In fact, in one case e-beam evaporated a-Si was found to exhibit no plateau region at all.³

Last, we report our measurement of α for 50 GHz ultrasound in the nc-Si:H sample whose deposition method was described above. We find a much larger value: $\alpha = 2600 \pm 660 \text{ cm}^{-1}$. While the literature does not contain measurements or calculations of acoustic attenuation in polycrystalline films in the GHz regime, the attenuation of ultrasound in the MHz range in polycrystalline media and its dependence on grain size and frequency have been thoroughly reviewed. If we consider that at 50 GHz in Si our measurement lies in the Rayleigh scattering regime ($\lambda \gg D$), then for cubic crystals the attenuation α is given by an expression $\alpha = Vf^4S$, where V is the average volume of a crystallite, f is the frequency of the ultrasound, and S is a Rayleigh scattering factor with units of dB/(MHz⁴ cm⁴) that is calculated from the density, sound

velocities, and elastic moduli of the material. For longitudinal waves in silicon, S has a numerical value of 42.5,³⁴ and to produce the attenuation we have measured at 50 GHz (22 580 dB/cm) we find that 44-nm-diameter crystallites are predicted. In practice, the crystal structure in nc-Si:H films is much more complicated than the simple picture suggested by Eq. (2) could describe. Combining Raman, XRD, AFM, and X-TEM measurements, nc-Si:H materials are normally considered as a mixture of small size nanocrystallites with a size of 20-30 nm embedded in an amorphous matrix, but the small nanocrystallites have the tendency to aggregate and form clusters with size of 0.5 μm .³⁵ Although the 44 nm crystallite size is slightly larger than the estimation from XRD, it is a very reasonable value, especially considering the effect of crystalline aggregation.

In summary, we have used picosecond ultrasonics to measure the attenuation of 50 GHz and 100 GHz ultrasound in a-Si:H and nc-Si:H films. We find the attenuation in a-Si:H at these frequencies to be much lower than other amorphous materials and lower than theoretical predictions based on anharmonic interactions. We also find that the attenuation in nc-Si:H at 50 GHz is nearly an order of magnitude higher than for a-Si:H.

This work was supported by NSF Award DMR-0906753 (Vassar College) and by the DOE under the Solar America Initiative Program Contract No. DE-FC36-07 GO 17053 (United Solar).

-
- ¹J. Fabian and P. B. Allen, *Phys. Rev. Lett.* **82**, 1478 (1999).
²D. G. Cahill, M. Katiyar, and J. R. Abelson, *Phys. Rev. B* **50**, 6077 (1994).
³B. L. Zink, R. Pietri, and F. Hellman, *Phys. Rev. Lett.* **96**, 055902 (2006).
⁴P. B. Allen and J. L. Feldman, *Phys. Rev. Lett.* **62**, 645 (1989).
⁵X. Liu *et al.*, *Phys. Rev. Lett.* **102**, 035901 (2009).
⁶H. S. Yang *et al.*, *Phys. Rev. B* **81**, 104203 (2010).
⁷G. Yue, B. Yan, J. Yang, and S. Guha, *Mater. Res. Soc. Symp. Proc.* **989**, 359 (2007).
⁸B. Yan G. Yue, J. Yang, S. Guha, D. L. Williamson, D. Han, and C.-S. Jiang, *Appl. Phys. Lett.* **85**, 1955 (2004).
⁹B. Yan *et al.*, *Mater. Res. Soc. Symp. Proc.* **1066**, 61 (2008).
¹⁰C. Thomsen, H. T. Grahn, H. J. Maris, and J. Tauc, *Phys. Rev. B* **34**, 4129 (1986).
¹¹G. A. Antonelli, B. Perrin, B. C. Daly, and D. G. Cahill, *MRS Bull.* **31**, 607 (2006).
¹²C. J. Morath and H. J. Maris, *Phys. Rev. B* **54**, 203 (1996).
¹³D. R. Lide (ed.), *Handbook of Chemistry and Physics*, 78th ed. (CRC Press, Boca Raton, FL, 1997).
¹⁴D. L. Williamson, *Sol. Energ. Mat. Sol. C* **78**, 41 (2003).
¹⁵W. Senn, G. Winterling, and M. Grimsditch, in *Physics of Semiconductors 1978*, ed. B. L. H. Wilson, (Institute of Physics, London, 1979), p. 709.
¹⁶A. Devos *et al.*, *Phys. Rev. B* **77**, 100201(R) (2008).
¹⁷R. O. Pohl, X. Liu, and E. Thompson, *Rev. Mod. Phys.* **74**, 991 (2002).
¹⁸B. C. Daly, K. Kang, Y. Wang, and D. G. Cahill, *Phys. Rev. B* **80**, 174112 (2009).
¹⁹J.-Y. Duquesne and B. Perrin, *Phys. Rev. B* **68**, 134205 (2003).
²⁰R. Vacher *et al.*, *Phys. Rev. B* **74**, 012203 (2006).
²¹C. Masciovecchio *et al.*, *Phys. Rev. Lett.* **92**, 247401 (2004).
²²R. Vacher, E. Courtens, and M. Foret, *Phys. Rev. B* **72**, 214205 (2005).
²³R. C. Zeller and R. O. Pohl, *Phys. Rev. B* **4**, 2029 (1971).
²⁴G. Baldi *et al.*, *Phys. Rev. B* **77**, 214309 (2008).
²⁵G. Baldi, V. M. Giordano, G. Monaco, and B. Ruta, *Phys. Rev. Lett.* **104**, 195501 (2010).
²⁶A. Akhieser, *J. Phys. (USSR)* **1**, 277 (1939).
²⁷H. J. Maris, in *Physical Acoustics*, edited by W. P. Mason and R.N. Thurston (Academic Press, New York, 1971), Vol. 8.
²⁸J. Fabian and P. B. Allen, *Phys. Rev. Lett.* **79**, 1885 (1997).
²⁹A. A. Bulgakov, V. V. Tarakanov, and A. N. Chernets, *Sov. Phys. Solid State* **15**, 1280 (1973).
³⁰J. M. Gibson *et al.*, *Phys. Rev. Lett.* **105**, 125504 (2010).
³¹S. Alexander, C. Laermans, R. Orbach, and H. M. Rosenberg, *Phys. Rev. B* **28**, 4615 (1983).
³²S. Alexander, O. Entin-Wohlman, and R. Orbach, *Phys. Rev. B* **34**, 2726 (1986).
³³A. Jagannathan, R. Orbach, and O. Entin-Wohlman, *Phys. Rev. B* **39**, 13465 (1989).
³⁴E. P. Papadakis, *J. Acoust. Soc. Am.* **37**, 703 (1965).
³⁵B. Yan *et al.*, *J. Appl. Phys.* **101**, 033711 (2007).